Neuromorphic Signal Classification Using Organic Electrochemical Transistor Array and Spiking Neural Simulations

Mahdi Ghazal, Ankush Kumar, Nikhil Garg, Sébastien Pecqueur, and Fabien Alibart

***Abstract*—Neuromorphic computing is an exciting and rapidly growing field that aims to create computing systems that can replicate the complex and dynamic behavior of the human–brain. Organic electrochemical transistors (OECTs) have emerged as a promising tool for developing such systems due to their unique bioelectronic properties. In this article, we present a novel approach for signal classification using an OECT array, which exhibits multifunctional bioelectronic functionality similar to neurons and synapses linked through a global medium. Our approach takes advantage of the intrinsic device variabilities of OECTs to create a reservoir network with variable neuron-time constants and synaptic strengths. We demonstrate the effectiveness of our approach by classifying surface-electromyogram (s-EMG) signals into three hand gesture categories. The OECT array performs efficient signal acquisition by feeding signals through multiple gates and measuring the response to a group of OECTs with a global liquid medium. We compare the performance of our approach with and without projecting the input on OECTs and observe a significant increase in classification accuracy from 40% to 68%. We also examined how the classification performance is affected by different selection strategies and numbers of OECTs used. Finally, we developed a spiking neural network-based simulation that mimics the OECTs array and found that OECT-based classification is comparable to the spiking neural network-based approach. Our work paves the way for the next generation of low-power, real-time, and intelligent biomedical sensing systems.**

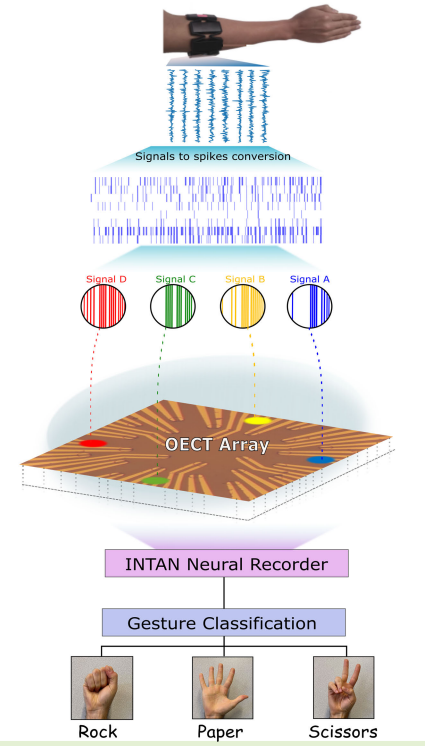

***Index Terms*—Biosensors, neuromorphic computing, organic electrochemical transistor (OECT), spiking neural networks.**

Manuscript received 30 September 2023; revised 20 December 2023; accepted 21 December 2023. Date of publication 15 January 2024; date of current version 14 March 2024. This work was supported by the European Research Council (ERC)-CoG IONOS Project under Grant 773228. The associate editor coordinating the review of this article and approving it for publication was Dr. Vinay Chakravarthi Gogineni. *(Mahdi Ghazal and Ankush Kumar contributed equally to this work.) (Corresponding authors: Ankush Kumar; Fabien Alibart.)*

Mahdi Ghazal and Sébastien Pecqueur are with CNRS, Centrale Lille, UMR 8520-IEMN, Université de Lille, Université Polytechnique Hauts-de-France, F59000 Lille, France.

Ankush Kumar was with CNRS, Centrale Lille, UMR 8520-IEMN, Universite de Lille, Universite Polytechnique Hauts-de-France, F59000 Lille, France. He is now with the Singapore University of Technology and Design (SUTD), Singapore (e-mail: ankush.kumar@univ-lille.fr).

Nikhil Garg and Fabien Alibart are with CNRS, Centrale Lille, UMR 8520-IEMN, Université de Lille, Université Polytechnique Hauts-de-France, F59000 Lille, France, and also with the Laboratoire Nanotechnologies and Nanosystèmes (LN2), CNRS, Université de Sherbrooke, Sherbrooke, QC J1X 0A5, Canada (e-mail: fabien.alibart@univ-lille.fr).

Digital Object Identifier 10.1109/JSEN.2024.3353307

I. Introduction

SIGNAL classification is a contemporary challenge, particularly in the domains of human–computer interface, medical science, and robotics, wherein the body signals are recorded and analyzed to infer the state of the body's activities [1], [2], [3], [4]. Artificial intelligence has made significant strides in efficient signal classification, with high accuracy rates, by leveraging sophisticated machine learning algorithms. However, despite these advancements, neural network-based classification still has limitations regarding energy consumption and compatibility with edge computing devices.

In contrast, the brain consumes several orders of lower energy due to its unique approach to spatiotemporal signal processing. In the brain, neurons effectively integrate parallel information from different spatial points (i.e., preneurons),

in which spike timing is a major component. To address this challenge, there is a growing need for multifunctional bioelectronic devices that could gather signal acquisition and amplification and contribute to feature extraction and classification [5], [6]. Organic electrochemical transistors (OECTs) have shown promising results as potential state-of-the-art devices for biosensing and neuromorphic applications, offering a new direction for signal classification research [7], [8], [9], [10], [11], [12], [13].

To enable the next generation of IoT devices, sensors must not only record data but also perform some computing functions. Thanks to the unique property of mixed conduction (ionic and electronic), OECTs can offer synaptic plasticity at various scales based on ionic and electronic charge transport mechanisms [14], which can be used to amplify signals of a particular frequency and remove signals of irrelevant nature [15]. The OECTs exhibit neuromorphic functions based on their temporal dynamics [16]. These attributes can be important in establishing next-generation non-Von-Neumann architecture devices, wherein the memory and computational unit can co-exist similarly to synapses in the brain. OECTs resemble neurons and synapses in their ability to transmit electrical signals and can be modulated by external factors. The electrochemical doping and de-doping process in OECTs is similar to the neurotransmitter release and uptake at the synaptic cleft, both involving controlled ion flow to modulate system behavior [16], [17].

OECTs are specifically chosen due to their distinct iono-electronic properties, which offer a unique temporal dimension that encompasses both ionic and electronic processes. The selection of OECTs as a key element is underpinned by the distinctive properties of the semiconductor channel, typically composed of PEDOT: PSS. PEDOT:PSS-based OECTs can achieve transconductance in the millisiemens range with response times within the microsecond range. The temporal dynamics of OECTs, coupled with the ability to modulate their behavior through electrochemical doping and de-doping processes, make them well-suited for applications requiring neuromorphic functionalities and biosensors where spatiotemporal signal processing plays a significant role in achieving high-performance sensing. Acknowledging nuanced considerations with PEDOT:PSS is crucial due to its direct impact on electrical properties, governed by the volume fraction of PEDOT influenced by the bulkiness of the PSS component. This interplay significantly guides the OECT channel material design based on the packing of the crystalline polymer morphology and the ionic mobility within the polymer film. This property emphasizes their adaptability for material engineering providing a platform for molecular engineering. Recent advances in material engineering have addressed these challenges by techniques such as side-chain attachment and backbone engineering to fine-tune the properties of the polymer material. The adaptability in material design is a key advantage, allowing for customization based on the requirements of different biosensing applications.

In addition, the commonly employed strategies for fabricating Poly(3,4-ethylenedioxythiophene) doped with poly(styrene sulfonate) (PEDOT: PSS) OECTs are via wet coating processes that maintain severe top-down limitations for downscaling and difficulty in modulating the device characteristics leading into variability in performances of different OECT devices implemented in one array. We propose to take advantage of this intrinsic variability of OECT property and apply it to the bio-signal classification approach, in which variability of neurons and synapse characteristics helps in the effective transformation of the signal by projecting input signals onto a higher dimensional space. Reservoirs represent a useful tool to improve signal classification based on this spatiotemporal projection with a simple read-out layer [18], [19]. In this manuscript, by capitalizing on the intrinsic behavior of OECTs, we determine the highly variable performances (i.e., time scale behavior and transconductance) of OECTs in an array system and turn it into an advantage to perform sensing and classification of electromyogram (EMG) biological signals. We utilized a dataset of surface-EMG (s-EMG) spiking signals obtained for three different hand gesture classes [20]. Using an INTAN setup, a multi OECTs network is used to sense the projected input signals from the source-drain characteristics of each individual device. The common electrolyte of the OECTs array is used as a shared medium and enables the coupling of the different input signals [21].

We compare the response of different OECTs for signals fed at different gates and use the integrated signal as feature vectors for classifying three different hand gestures. A specific number of trials are used for training the classifier, and the task classification accuracy is evaluated on the test data. Multiple groups of OECTs are compared for classification accuracy, and maximum accuracy is identified for OECT arrays. This network achieved 66% accuracy with 13 OECTs, compared to 39% accuracy from the raw signals, highlighting the important role of feature extraction by OECTs as artificial neurons in effective signal classification.

OECTs essentially function like neurons, featuring a specific time constant of integration and variable synaptic strengths, owing to variable distances. The OECT network aids in projecting signals into higher-dimensional spaces, enhancing the separability of features. Furthermore, OECT network filtering contributes to the refinement of temporal signal characteristics.

However, OECTs exhibit device-to-device variability, prompting us to investigate whether such variability, even when induced with randomness in weight and time constant, can be accommodated in bio-sensing. Brain-inspired neural networks, or spiking neural networks, do similar computations with the help of trainable weights and LIF neurons. The LIF neurons do a low pass filtering on the signal before applying the non-linearity (spikes). To understand where the better performances of the OECTs projection come from, we design a spiking neural network simulation with a variable time constant and weights; a spiking neural network-based simulation is developed, which mimics the OECTs array and provides further insights.

II. Experimental Methods

A. OECT Microfabrication

The OECT arrays consist of glass slides (5×5 cm^2) which are patterned with gold metallic lines forming the sources and drains electrodes. PEDOT: PSS (Clevios[1] PH1000) were coated, forming the OECT channel between the source and the drain. All chemicals were purchased from Sigma Aldrich. The OECTs were insulated by a parylene-C layer. The resulting W/L for OECTs was 30/12 μm.

B. Electrochemical Impedance Spectroscopy

The EIS measurements were performed with a Solartron Analytical (Ametek) impedance analyzer from 1 MHz to Hz in PBS as an aqueous solution. All impedance measurements were done in the same electrical conditions where the source and the drain as working electrodes and grounded Ag/AgCl wire as a reference electrode dipped into the electrolyte.

An open-source EIS Spectrum Analyzer software was used to perform circuit impedance modeling. The resistance and capacitance parameter fitting were manually adjusted by simultaneous comparison of Bode's modulus, Bode's phase, and Nyquist plots.

C. DC Electrical Characterization

Agilent B1500A semiconductor device analyzer was used to bias the transistor and record the output drain current. The OECTs were characterized using a PBS solution as the electrolyte. An Ag/AgCl wire was used as the gate electrode and immersed in the electrolyte.

D. INTAN Parallel Readout

The "RHS2000 INTAN 128ch" Stimulation/Recording controller is a system that allows users to record potential signals up to 128. This device contains four ports providing connection points for the stim/record headstages; each headstage contains 32 channel amplifier chips. Each stim/record headstage contains one or two RHS2116 amplifier chips. Each channel includes a low-noise amplifier with a programmable bandwidth. While we use OECTs with drain output current, some electronic setup was implemented to make this INTAN device compatible with the OECT array. This electronic setup was composed just of passive devices in order to achieve compatibility between OECT and INTAN [Figs. 1(d) and 2(a)]. The aim is to implement a voltage divider circuit setup for each OECT in the array to get voltage outputs so it can be compatible with measurements using this INTAN device. The REF pin of the headstage is shorted and connected to the ground of its amplifier by connecting the REF pin to the circuit's ground, the output voltage of each voltage divider setup at each electrode pin. All the recorded signals are applied with a bandpass filter from 10 to 1000 Hz.

E. Classification

The classification is studied on the publicly available Roshambo dataset [20] collected through the Myo armband (eight locations) for three hand gestures (rock, paper, and scissors) for ten participants across three sessions. The total experimental set of 150 datasets is divided into multiple combinations of training dataset (100) and test dataset (50). The continuous time series (eight signals coming from eight EMG sensors) are converted into discrete spike trains using a temporal contrast method [22]. Herein, the spike is generated if the difference between successive values exceeds a predefined threshold. The eight signals are converted into 16 signals based on positive and negative thresholds.

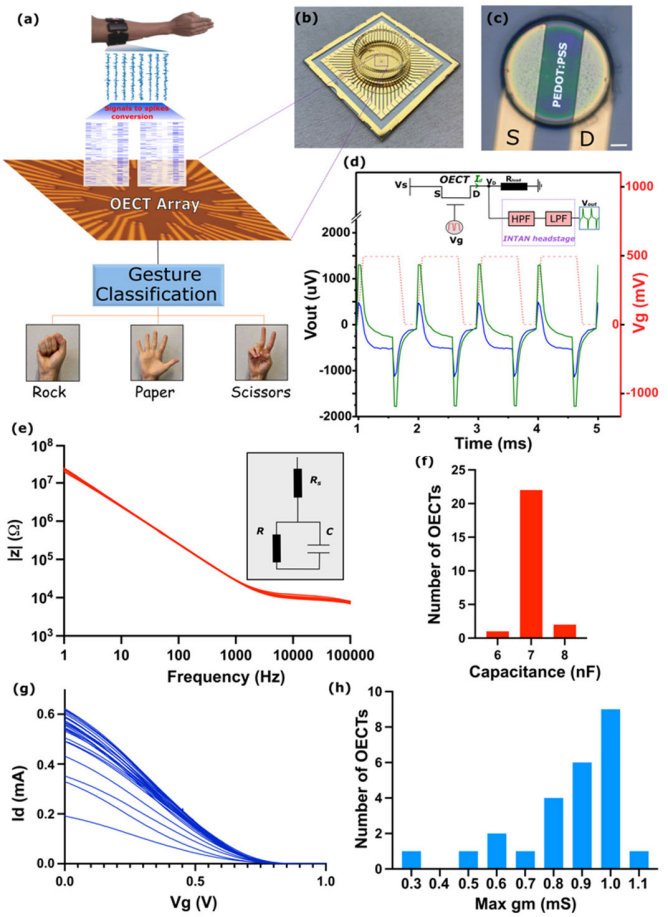

Fig. 1. (a) Schematic representation of utilization of OECT array for signal classification. Analog s-EMG signal from an armband is recorded during various hand gestures. The obtained analog signal is then converted into spike trains and is fed to the OECT array. The measured time series on the OECT array is used for signal classification applications, such as specific hand gestures. (b) Photograph of a multielectrode system with 24 electrodes consisting of four gates and remaining OECTs. (c) A single sensor consists of two Au electrodes acting as the source and drain with PEDOT deposition between them acting as the OECT (scale bar: 5 μm). (d) Typical characteristics of two different OECTs (blue and green) with different behaviors to a square pulse of width 0.6 and 0.1 ms rise and fall time applied through the gate. Prior to the recording, the measured signal is passed through high pass and low pass filters using INTAN RHS2116 headstage amplifier chips. (e) Bode plot curve showing the impedance modulus of multiple OECT ($n = 25$) from the same chip. Inset: equivalent electrical circuit is used to model the impedance spectroscopy recorded through the OECTs. (f) Distribution of capacitance values extracted from the impedance Bode plot curve in (e). (g) Transfer characteristic curves of the same OECTs represented in (e). (h) Distribution of the maximum transconductance (mS) of the OECTs.

[1]Trademarked.

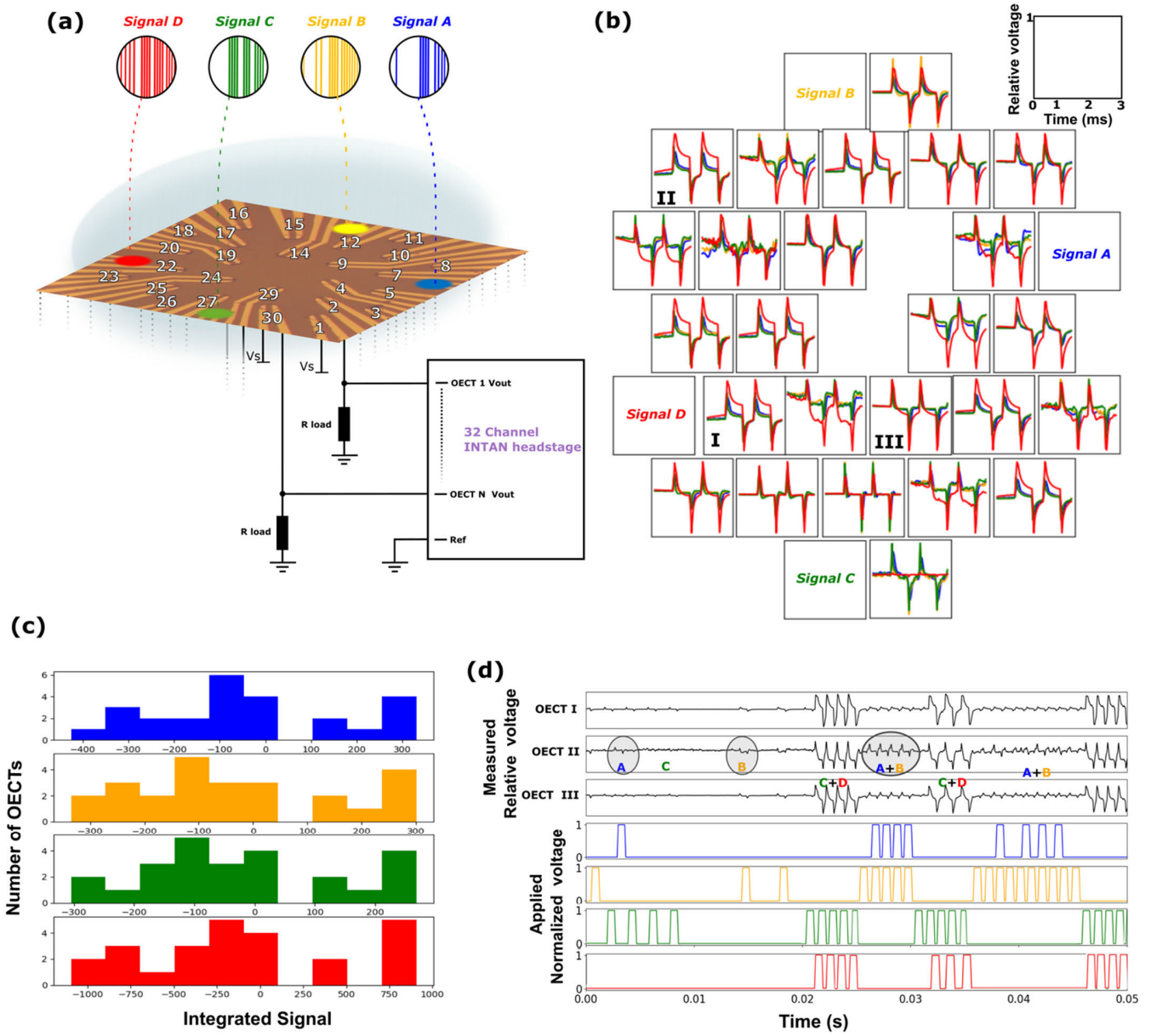

Fig. 2. (a) Representation of OECT measurements for various gate signals with the shared medium. Herein, various signals can be fed at different gates and measurements can be performed simultaneously for different OECTs. (b) Comparison of characteristics of OECTs for signals fed at different gates one by one. The sequential signals applied on different gates are represented with different colors and are plotted on the same time axis for comparison. (c) Histogram showing the integrated values of signals obtained from different OECTs over their complete duration. (d) Comparison of the characteristics of a few examples of OECTs on applying specific signals (shown in red, green, yellow, and blue) at different gates. The OECTs integrate signals from different gates through the global electrolyte.

The energy consumption of the spike encoder can be accounted for by static power dissipation and dynamic energy per spike. While the circuits for spike conversion are not discussed in this study, an implementation has been recently reported in the literature [23]. The spike conversion circuit is essentially composed of a signal conditioning chain, and an event generator. The event generator mainly compares the output of signal processing chain to a fixed threshold and produces an output spike. Conventional CMOS is the ideal choice for this spike generator/comparator. However, the signal conditioning chain could potentially be replaced by OECTs by exploiting the *RC* filtering capabilities of these network. Nevertheless, in this study, the spike conversion is performed in software.

Due to experimental limitations of the source meter, we could only provide four parallel signals simultaneously to the gates. Hence, out of 16 signals, four signals were selected based on random forest algorithms with higher feature importance. These four signals are denoted as “raw signals” for convenience. We use three methodologies for classification: 1) classification using raw signals; 2) classification using recorded signals on OECTs; and 3) classification based on spiking neural network simulations by feeding the raw signals. For accurate comparison, in all the cases, the ratio of training

and testing data is maintained the same, and classification is performed with random forest algorithms with similar hyperparameters. In first cases, the classification using raw signals is performed by integrating the signals of complete duration and using integrated value as a feature vector.

In the second case, the classification with OECT arrays is performed utilizing N-selected output signals from the OECTs. The integrated amplitude response for the time duration is considered as the feature vector. The selection of OECTs is done randomly or based on the individual best performance in classification.

To mimic the effect of the OECTs network on signal classification, Spiking Neural Network simulation is performed in which artificial neurons act as LIF filters similar to OECTs and, synapsis acts as a global medium. The spiking neural network simulations are performed on Brian 2.0 by designing input layers with four neurons receiving the raw binary signal, connected to LIF hidden layer neurons. The spiking rate of the hidden neurons is used as the feature vectors. Further, a similar random forest algorithm is applied to train and classify the data. For a systematic study, the input-hidden neuron synaptic strengths are varied from uniform to random values. To study the effect of randomness in the connection strength, the synaptic network is constructed with weight $W[i, j]$ from the input i to hidden layer j as $W[i, j] = C_1\ W_0 + C_2$ rand(), with C_2 coefficient deciding the random component and $C_1 + C_2 = 1$. Further, the neurons' integration time constant is also systematically varied from 2 to 20 ms for the random network case. Additionally, we examined the classification as a function of neuron time constant values based on the uniform distribution in the time constant values. The accuracy in each network case is determined for five different sets of training and testing data and are plotted in Fig. 4(b) and (c).

III. Results and Discussions

In Fig. 1(a), we present a concise overview of our data acquisition and signal classification methodology using the OECT array. Each spike corresponds to a square pulse with a width of 0.6 ms and rise and fall times of 0.1 ms. These signals are directed into common gates for subsequent measurement of OECT characteristics. Fig. 1(b) and (c) show the OECT arrays having Au source (S) and drain (D) electrodes spaced by 12 μm, and PEDOT: PSS of 200 nm was deposited using the spin-coating technique. Spin-coating is carried out at room temperature and ambient atmosphere conditions, which could cause significant variations in the electronic mobility of the PEDOT: PSS channel of multiple OECTs within the same array [15]. The variability in the mobility values of different OECTs implemented in one array chip will induce variability in the following two different important performance characteristics of an OECT:

1) Transconductance (gm), which gauges an OECT's ability to amplify an input signal from its channel using gate voltage. This parameter depends on factors such as electrode geometry and material properties, including mobility.
2) Response time, indicating the speed of an OECT's signal response. The electronic transient response (τe) is directly linked to the OECT's mobility value, while the ionic transient response (τi) is influenced by the channel's capacitance [9], [14]. Inherent variabilities cause all OECTs to incorporate different time and voltage features in response to the pulsed gate signal. To assess this concept, Fig. 1(d) presents the transient responses of two OECTs from the same array with varying mobility values, subjected to 500 mV and 1 ms pulses via a common Ag/AgCl gate wire immersed in the electrolyte. As depicted, due to inherent variability during fabrication, both devices exhibit distinct dynamic responses in terms of amplitude and timing.

Beyond the intrinsic variability, another factor influencing OECT transient response is the gate's material and its proximity to the OECT. The ionic transient response (τi) in the electrolyte is governed by factors such as the solution resistance and the ionic double layer. It adheres to electrolyte relaxation kinetics dependent on ionic transport between the gate and the OECT [24], Consequently, it varies with the electrolyte's resistance, gate material (capacitance), and the distance between the OECT and the position of an emitting gate [14], [24].

Fig. 1(e) displays the Bode's modulus plot showing impedance spectra measurements ranging from 1 Hz to 1 MHz in an electrolyte containing phosphate-buffered saline (PBS) solution for a set of 25 OECTs from the same array. Electrochemical impedance spectroscopy (EIS) modeling was employed to extract key electrical parameters, including the capacitance of the OECT and the electrolyte resistance. The equivalent circuit, as depicted in the inset of Fig. 1(e), served as the foundation for this modeling effort.

Within the impedance modulus, the quasi-plateau region represents the solution resistance (Rs), while the initial portion of the impedance modulus at low frequencies is described by a resistor-capacitor circuit (R and C). This model adheres to the typical simplified representation employed to characterize the electrode-electrolyte impedance.

Fig. 1(f) presents a histogram depicting the distribution of extracted OECT capacitance values obtained from the impedance measurements. An additional critical parameter derived from this model, which can impact the transient response of an OECT, is the electrolyte resistance, maintaining a consistent value of approximately 10 kΩ (a common electrolyte). In Fig. 1(g), the transfer curve for the same OECTs characterized in Fig. 1(e) is presented. Examining the histogram displaying the distribution of maximum transconductance (gm) values in Fig. 1(h) for these OECTs reveals an initial substantial variability in transconductance, with a standard deviation of approximately 25%. This stands in contrast to the relatively minor variability in capacitance, as shown in Fig. 1(f) (standard deviation of approximately 4%). These observations suggest that the primary source of variability in transconductance lies in mobility rather than capacitance. Furthermore, this variability in mobility values is expected to manifest as variability in the response time across all OECTs within the same array.

For reservoir computing applications, the spatio-temporal responses of OECT arrays are analyzed systematically for time-dependent signals. Fig. 2(a) demonstrates the recording of OECT arrays with multiple terminal inputs. Various signals can be applied at the four different gates and responses from different OECTs can be measured. First, for comparing the response of different OECTs, the same periodic signals [similar to Fig. 1(d)] are fed successively at different gates, and responses are monitored at various OECTs. Fig. 2(b) shows the spatio-temporal response on a single plot to compare signals fed through different gates. All the OECTs are in the same liquid medium with variable gate-OECT distances, offering parallel coupling, shared information, and spatiotemporal responses. Due to differences in materials and fabrication variability, the intrinsic resistance of different OECTs (sensor and gate) is variable. Therefore, the gate material, gate-OECTs distances, and mainly the variability in the nature of sensing-OECTs (i.e., variability in transconductance presented in Fig. 1) contribute to variable responses. Both the electronic and capacitive currents are observed in these devices with different strengths [26], [27]. In most cases, the OECTs closer to specific gates offer a higher response as compared to OECTs located further away. Fig. 2(c) shows the response of several OECTs when a typical EMG spike signal is fed at all gates. Signals A–D reflect the typical nature of signals, exhibiting nonuniform firing rates and correlated activities between inputs at specific times. As a result, the effective gate voltages are variable, leading to variable amplitude responses. For example, signals fed from gate C have comparatively higher amplitude response on OECTs arrays. Furthermore, OECTs exhibit higher amplitude during the correlated spiking events and exhibit the effect of correlation-based firing. A few example cases are discussed with individual and correlated firing. As indicated, the response is higher when A and B are firing together as compared to individual firing (marked with gray circle in Fig. 2(d).

Further, the measured signal amplitude also depends on the relative spike-time difference of individual signals; as an example, the correlated firing of C and D shows different characteristics at two different time durations [see Fig. 2(d)]. In this way, the information from different gate signals and their coincidence gets translated into the characteristics of OECT.

The variability of OECTs and their spatiotemporal characteristics can be utilized as a reservoir network for signal classification. We conducted experiments for s-EMG signal classification to explore these characteristics using OECTs, as shown in Fig. 3 (refer to methods for details). The importance of 16 spiking channels was evaluated through random forest-based classification with rate-based feature vectors. Out of 16 signals, the four most important signals are fed to the gates of OECTs, and their time-varying responses are monitored by the OECT arrays. The experiments consisted of 150 sets with known rock, paper, and scissor classes. We utilized 150 trial signals corresponding to three classes and measured the OECT array responses for each trial, with two-thirds of the data used for training the classifier and one-third for testing. We generated multiple sets of training and testing sets to calculate accuracies, and the mean accuracy and corresponding error are presented in the figure.

From a neural network perspective, the variation in the gate-OECT distances offers different strengths in the recording, similar to a fully connected neural network with variable weight values and neuron characteristics. Fig. 3(a) shows the schematic representation of utilizing the OECT as a neural network layer. The OECT integrates the current from different gates using the common electrolyte, and the integrated amplitude of the OECT for the whole-time duration of the trial serves as a feature for classification, with each OECT corresponding to an individual feature vector. By computing the integral (summation of time series), we convert a vector of a big dimension into just one number.

While traditional synaptic devices exhibit specific weight-tuning characteristics, it is important to note that in our model, OECTs are conceptualized more as neurons than conventional synaptic devices. The learning aspect in this scheme is not explicitly driven by synaptic weight tuning, as in traditional neural networks. Instead, the learning dynamics emerge from the collective spatio-temporal responses of the OECT array to input signals. The OECTs act as complex nodes that integrate and transform signals, contributing to the overall performance of the system in a manner akin to synaptic interactions. This distinction is crucial for understanding the unique neuromorphic capabilities of the OECT array in signal classification tasks. The OECT network acts as a reservoir neural network while the readout layer is trained ex-situ by using the integrated time series response on different OECTs. By training the readout layer externally, the neural network is endowed with the ability to generalize patterns and features extracted from the OECT responses, contributing to the overall efficacy of the network in processing and interpreting complex datasets. We have two transformations occurring both within the reservoir network and one at the readout layer. The reservoir network, characterized by the OECT arrays, processes the temporal dynamics and summation of inputs with different weights. We have used a Random Forest classifier at the readout layer based on the integrated time series responses obtained from the OECT arrays. Rather than a Random Forest Classifier, one can, in principle, also explore SVM or LDA classifier which can be closer to vector-matrix multiplication operation.

We utilize N random feature vectors obtained from N random OECTs and calculate the classification accuracy with random forest classifiers on the test data. As shown in Fig. 3(c), the mean accuracy is below 40% for two OECTs, rises to nearly 60% for five OECTs, and shows maximum 66% accuracy for 13 OECTs. Thus, increasing the number of OECTs increases the accuracy of signal classification, and after an optimum number, there is no further accuracy enhancement.

Due to inherent variability among different OECTs, these devices may operate in different regimes and offer varying signal transformation properties. As a result, the performance of a group of OECTs may depend on each device's individual signal transformation characteristics. To illustrate this concept, the accuracy of an OECT array was measured for different

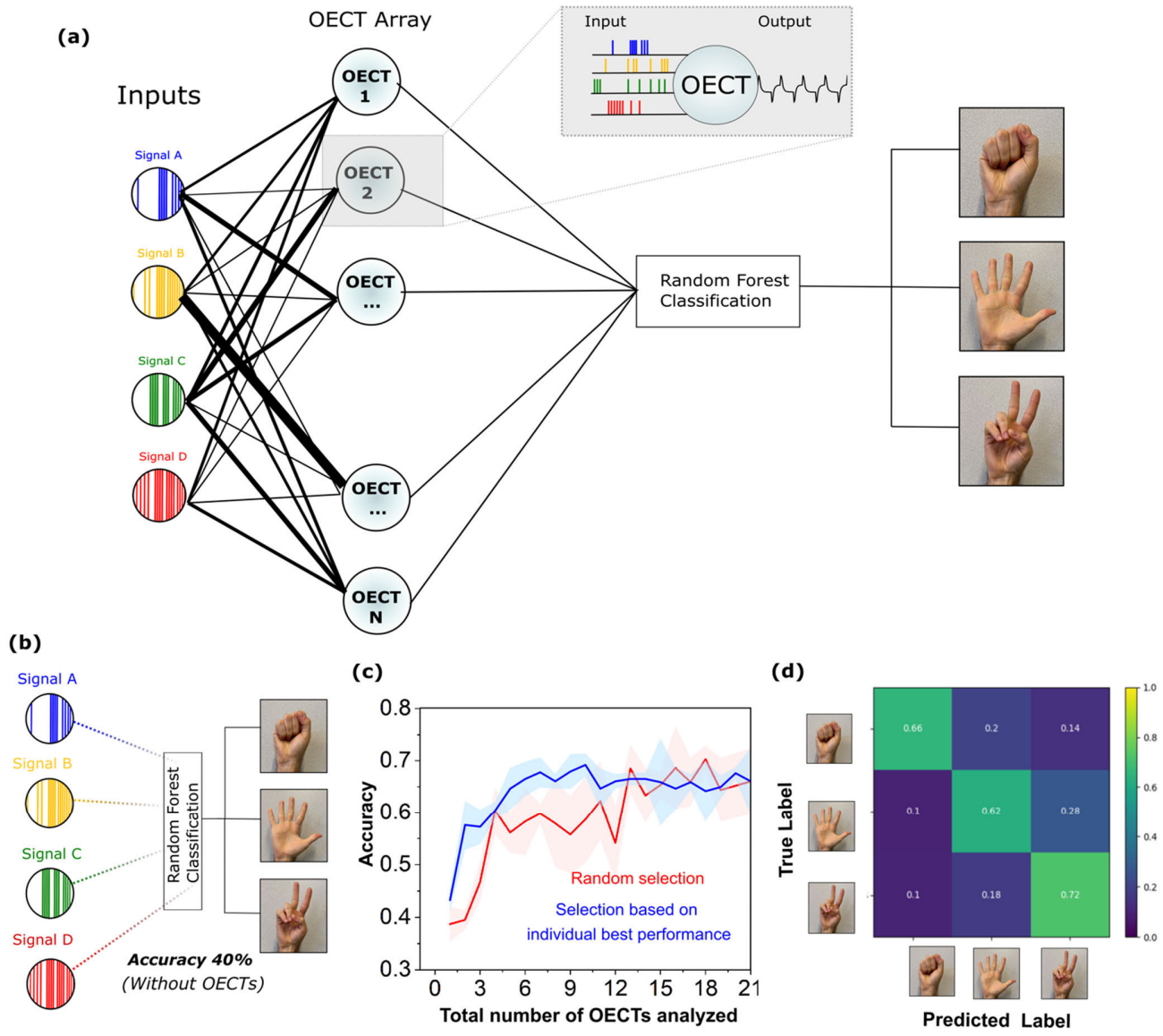

Fig. 3. (a) Schematic representation of utilizing the OECT array for signal classification. The OECT integrates the current from various gates. The rate-based coding is used for the classification. (b) Signal classification of raw spiking signals. (c) Accuracy comparison for various numbers of OECT arrays selected randomly (shown in red) and based on best individual performance (shown in blue). (d) Confusion matrix of classification with four OECTs.

OECTs individually. The results showed that various OECTs exhibited different accuracy values, ranging from 36% to 50%. To select the most effective group of OECTs for signal classification, an OECT list was created based on decreasing individual accuracy. The classification was then performed using multiple OECTs, with the best-performing individual devices selected for use. In this selection case, two OECTs achieved 58% accuracy, while nine OECTs achieved 68% accuracy. The confusion matrix of one of the best-selected cases is shown in Fig. 3(d). Therefore, individual OECT selection can be effective for group OECT selection, enhancing overall accuracy. This simple approach can be highly useful when dealing with a large number of available OECTs. However, more optimized OECTs selections can also be performed using genotic algorithms or similar approaches. Overall, the individual study of OECT classification properties can greatly improve signal classification accuracy. The application of bandpass filtering by INTAN may introduce a trade-off between noise reduction and the potential loss of relevant information. The other effect could be that at some point, additional OECTs are just increasing the redundancy and not the signal projection/features extraction. OECTs are different only to some extent and by adding more OECTs we only bring correlated or irrelevant information, thus not increasing accuracy further.

As a comparison control, random forest is used to measure the accuracy of the four raw spike signals [Fig. 3(b)], with accuracy found to be only 40%. The low accuracy offered by raw signals, compared to signals obtained through OECTs, reflects the efficient signal transformation character-

istics of OECTs. The classification using the raw signals, by using the integral of the signals, does not capture the time-variant non-uniformity and intercorrelation among the signals. On the other hand, the strength of OECTs lies in their ability to efficiently capture the non-uniformity of spikes and mutual correlation, which is essential in providing an effective feature vector for classification. To compare with state of art works, in our other publication, it was demonstrated that signal classification using support vector machines (SVMs) achieved 61% accuracy with 16 inputs, a metric that could be enhanced to 80% through optimized structural plasticity rules [28]. Furthermore, employing a Critical Reservoir in the state-of-the-art scenario optimized accuracies to 88% with 320 reservoir neurons [22]. It is noted that this work involves sensing and measurement, leading to the partial removal of important features, and limiting direct accuracy compared to state-of-art software approaches. In comparison, this work achieves an accuracy of 68% with only nine OECTs, utilizing four inputs and a reduced training dataset of 1/3rd.

As discussed, the OECT arrays offer integration of signals with specific time constants leading to an increase in conductance of OECTs with correlated signals, and different gate-OECT distance leads to variable weight contribution from signals generated from different gates. Moreover, the material characteristics of OECTs are different, which can lead to different time constants. Further, the characteristic gates also lead to different amplitude contributions. In a modeling platform, incorporating all the above variabilities cannot easily be mapped one to one. We utilize spiking neural network simulations to understand some of these effects controlling the OECT array behavior. OECTs offer integration capabilities similar to neurons, and the global medium offers a synaptic strength among different OECTs. Though the non-linearity in OECT and artificial neurons might not be the same, the underlying similarity is that both offer integration of current. A projection layer is a critical element within a neural network, responsible for transforming input data into a new feature space. Through the efforts of the OECTs controlled by multiple time series, the input data are transformed into a new feature space. The OECT offers time series transformation based on the integration of correlated signals. We generate a fully connected spiking neural network with inputs based on EMG spike signals. Two cases are considered: 1) constant connection weight between the layers and 2) random connection weight between the layers. The neurons in the second layer are leaky-integrate and fire neurons and offer non-linearity to the circuit by executing temporal integration, and synapses provide spatial integration. The postsynaptic neuron integrates the current from all incoming synapses from the first layer and fires only if the postsynaptic potential rises above a threshold (Fig. 4(a) inset). The firing rate of the neurons is used as a feature vector for the classification task utilizing a random forest classifier.

We compare the constant synaptic weight with random synaptic weight by systematically introducing random components in the constant weight. This approach reproduces the spatial integration properties of the OECTs array, where

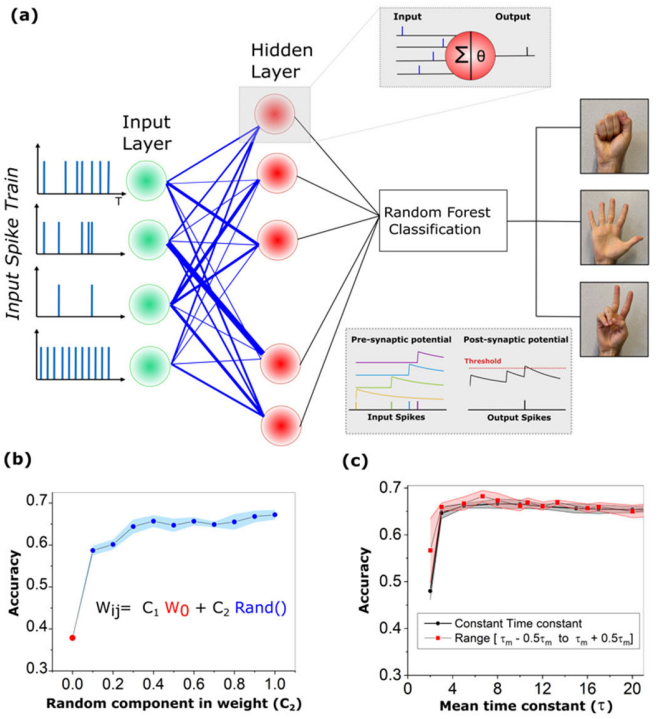

Fig. 4. (a) Signal classification based on spiking neural network simulations. The raw signal neurons (green) are connected to a hidden layer of neurons (shown in red). The connection strength between the input and hidden layer possesses certain weight values. The neurons in the hidden layer (see inset) integrate the current from presynaptic neurons and fire on exceeding the threshold. Rate-based coding is used with a random forest classifier for the accuracy comparison. (b) Accuracy comparison for input-hidden layer weights ($W[i, j]$) of varying random components as $W[i, j] = C_1\ W_0 + C_2$ rand(), with C_2 coefficient deciding the random component. (c) Accuracy comparison for neurons of variable values and distribution of time constant.

the response of OECTs differs for different gates due to variable spatial distances. The classification task is performed for several such networks individually, and the accuracy values are shown in Fig. 4(b). It is found that with a constant weight of the connection network, the accuracy is just 37%; on the other hand, with a small component of randomness (0.1) the accuracy rises to 59%. The classification improves with a systematic increase of random components and possesses a maximum value of 67% with the complete random case. Thus, the uniformity in the synaptic strengths has a huge role in increasing accuracy. The variable gate-OECT distances offers inherent non-uniformity in the gates-OECT synaptic strengths, which could be an important reason for their high accuracy. Moreover, we studied the classification as a function of neuron time constant values and based on the distribution in the time constant value [Fig. 4(c)]. The spiking network simulation with a variable time constant integrates signals of a particular duration. The accuracy is found to be significantly low, i.e., 47%, for the low time constant value. On the other hand, the accuracy is also found to be constant at a very high time constant (which integrates signal for a longer duration). The study reflects the role of integrating of optimum time duration of signal for effective feature extraction. Since the OECT fabrication techniques can help in adapt the time constant and

its distribution, one can design an OECT array for effective classification. In neurophysical recordings, many times the task is to record the signal from multiple cells and the task is to analyze the data based on the firing pattern. The present approach of recording the data through OECT arrays would help to record and analyze the data.

Noise is known to affect the reservoir computing accuracy due to overfitting of the data. OECTs can offer multiple noises such as $1/f$ noise due to fluctuations in charge at the surface and the bulk of the channel material [29]. Higher channel thickness might be the solution to achieve low $1/f$ noise values, which also provides high transconductance [30]. Based on a systematic study by Nathe et al. [31], the low pass filter reduces the error in classification. In our system, OECT offers inherent low pass filter properties with the cut-off frequency dependent on the RC of the OECTs. Consequently, OECT-based reservoir computing could provide an effective approach to enhancing accuracy. Moreover, we use the integral of the signal as the feature. For a significantly low white noise, the integral of the signal would have a low standard deviation due to large data points in the time series as a result, low values of white noise might not affect the accuracy significantly. Further, studies can be done to systematically optimize the OECTs for effective classification.

OECT has a remarkable capacity for precision in performance (capacitance and transconductance) control across a wide range, a feature primarily achieved through the manipulation of material engineering, with PEDOT: PSS playing a key role [32]. The biocompatibility of these systems also brings a special advantage to the brain–computer interface. In this study, we aim to specifically highlight the beyond CMOS strategy using these devices that use spatio-temporal pulse activity correlation on few number of nodes to retrieve an environmental activity induced by local voltage modulations, for which the complexity of the recognition is not strictly related to the number of voltage sensing input nodes, and therefore, the integration density of the OECT technology. As a proof of concept, we showed that such a theses micro-scaled devices (from as few as six OECT as shown in Fig. 3) are enough to recognize 4-D patterns of voltage-spikes to classify them into three different classes: the rock-paper-scissor test is obviously used as toy-problem to generalized our approach to any ternary classifications for other applications than the one we aim that would require gathering computing resources near-sensors out of CMOS. Also, as Fig. 3 suggests, the classification performances scale with the number of input nodes involved in the spike sorting to match the dimensional complexity of voltage patterns to sense. In many applications, information patterns can be emitted by more than four input gates to require more than six OECT inputs to sort any spike voltage pattern. Therefore, downscaling this technology for higher density integration is for sure an asset, despite the approach being beyond-CMOS. As electropolymerization is a bottom-up strategy, downscaling the OECT at the level of lithographically patterned metal lines is perfectly in line future needs to increase the number of sensing nodes while keeping the same computational resources on each of them.

Reservoir computing consists of converting input data into high-dimensional data through the reservoir which is a non-linear system. The training and testing of such systems purely through software can be computationally demanding, owing to the numerous connections within the network. It is followed by classification based on the spatiotemporal pattern of the reservoir states as the read-out layer. In this context, our proposed method leverages arrays of variable OECTs to harness the capabilities of a reservoir network via a global medium. This approach eliminates a significant computational burden that is typically associated with traditional software-based reservoir computing. Instead, we employ a straightforward summation of time series operations as a key feature for the classification process. Our analysis demonstrates that a relatively small number of OECTs, as few as nine in the case of EMG signal classification, can yield remarkably high accuracy when integrated into the read-out layer. Moreover, various techniques such as Basic Weighted Non-linear Transform and Winner Takes All can be employed effectively for edge computing applications.

Currently, values of weights and time constants are not identical for different OECTs. Our findings indicate that while OECT arrays and SNN simulations differ in their underlying mechanisms, the classification accuracy achieved by OECT arrays is statistically indistinguishable from that of the SNN simulations. This intriguing congruence between the bioelectronic behaviors of OECT arrays and the computational capabilities of SNNs underscores the potential of OECTs as an innovative and energy-efficient tool for signal classification in neuromorphic computing applications. The study helps in rethinking the sensing cum computing architecture for edge computing which would be needed for low-power applications. The OECT arrays can also be explored for spatio-temporal brain recording and task classification [7].

IV. Conclusion

In this study, we have demonstrated the efficacy of global medium-based OECT arrays as potent biosensors for signal classification. The interconnected network of OECTs significantly enhances the spatiotemporal pattern differentiability, akin to the principles underlying reservoir computing. Our experimental results reveal that the OECT array consistently achieves a classification accuracy of $\sim$70%, utilizing just nine OECTs, as compared to the more modest 40% accuracy obtained when working directly with raw signals.

The SNN simulation with randomly initialized weights was used to enhance the signal from OECT further. The spiking neural network simulation is performed to understand better classification tasks with variable degrees of random weights and neuron's time constant. Future work can utilize these devices for neuron recording and classification tasks based on neurons' firing patterns. Looking ahead, the promising outcomes of this research pave the way for a multitude of exciting possibilities. These multifunctional bioelectronic devices, leveraging the inherent variability of OECT properties, hold potential not only for signal classification but also for neuron recording and classification tasks centered

around the intricate firing patterns of neurons. To assess the viability of OECTs for interfacing with real neurons, key considerations include sensitivity for detecting subtle changes in neuronal signals, fast response time, a high signal-to-noise ratio (SNR) for clear signal distinction, specificity in isolating neuronal signals from background noise, biocompatibility to prevent adverse reactions, long-term stability, and adaptability to diverse neural networks. Evaluation of these factors provides insights into the potential applications and limitations of OECTs in neurotechnology. By harnessing the unique characteristics of OECTs, we anticipate that future work will propel the development of advanced neuromorphic systems that can mimic and understand neural processing with unparalleled precision.

Acknowledgment

The authors would like to thank RENATECH network and the engineers from IEMN for their support.

References

[1] Y. Cho, S. Park, J. Lee, and K. J. Yu, "Emerging materials and technologies with applications in flexible neural implants: A comprehensive review of current issues with neural devices," *Adv. Mater.*, vol. 33, no. 47, Nov. 2021, Art. no. 2005786, doi: 10.1002/adma.202005786.

[2] F. Torricelli et al., "Electrolyte-gated transistors for enhanced performance bioelectronics," *Nature Rev. Methods Primers*, vol. 1, no. 1, p. 66, Oct. 2021, doi: 10.1038/s43586-021-00065-8.

[3] E. Gokgoz and A. Subasi, "Comparison of decision tree algorithms for EMG signal classification using DWT," *Biomed. Signal Process. Control*, vol. 18, pp. 138–144, Apr. 2015, doi: 10.1016/j.bspc.2014.12.005.

[4] F. Corradi and G. Indiveri, "A neuromorphic event-based neural recording system for smart brain–machine-interfaces," *IEEE Trans. Biomed. Circuits Syst.*, vol. 9, no. 5, pp. 699–709, Oct. 2015, doi: 10.1109/TBCAS.2015.2479256.

[5] C. Koch, *Biophysics of Computation: Information Processing in Single Neurons*, 1st ed. London, U.K.: Oxford Univ. Press, 2004.

[6] L. F. Abbott and W. G. Regehr, "Synaptic computation," *Nature*, vol. 431, no. 7010, pp. 796–803, Oct. 2004, doi: 10.1038/nature03010.

[7] D. Khodagholy et al., "In vivo recordings of brain activity using organic transistors," *Nature Commun.*, vol. 4, no. 1, p. 1575, Mar. 2013, doi: 10.1038/ncomms2573.

[8] D. Khodagholy et al., "High transconductance organic electrochemical transistors," *Nature Commun.*, vol. 4, no. 1, p. 2133, Jul. 2013, doi: 10.1038/ncomms3133.

[9] J. Rivnay, S. Inal, A. Salleo, R. M. Owens, M. Berggren, and G. G. Malliaras, "Organic electrochemical transistors," *Nature Rev. Mater.*, vol. 3, no. 2, p. 17086, Jan. 2018, doi: 10.1038/natrevmats.2017.86.

[10] P. Gkoupidenis, N. Schaefer, B. Garlan, and G. G. Malliaras, "Neuromorphic functions in PEDOT: PSS organic electrochemical transistors," *Adv. Mater.*, vol. 27, no. 44, pp. 7176–7180, Nov. 2015, doi: 10.1002/adma.201503674.

[11] C. Yao, Q. Li, J. Guo, F. Yan, and I. Hsing, "Rigid and flexible organic electrochemical transistor arrays for monitoring action potentials from electrogenic cells," *Adv. Healthcare Mater.*, vol. 4, no. 4, pp. 528–533, Mar. 2015, doi: 10.1002/adhm.201400406.

[12] K. Janzakova, M. Ghazal, A. Kumar, Y. Coffinier, S. Pecqueur, and F. Alibart, "Dendritic organic electrochemical transistors grown by electropolymerization for 3D neuromorphic engineering," *Adv. Sci.*, vol. 8, no. 24, Dec. 2021, Art. no. 2102973, doi: 10.1002/advs.202102973.

[13] M. Ghazal, T. Dargent, S. Pecqueur, and F. Alibart, "Addressing organic electrochemical transistors for neurosensing and neuromorphic sensing," in *Proc. IEEE SENSORS*, Montreal, QC, Canada, Oct. 2019, pp. 1–4, doi: 10.1109/SENSORS43011.2019.8956648.

[14] D. A. Bernards and G. G. Malliaras, "Steady-state and transient behavior of organic electrochemical transistors," *Adv. Funct. Mater.*, vol. 17, no. 17, pp. 3538–3544, Nov. 2007, doi: 10.1002/adfm.200601239.

[15] M. Ghazal et al., "Bio-Inspired adaptive sensing through electropolymerization of organic electrochemical transistors," *Adv. Electron. Mater.*, vol. 8, no. 3, Mar. 2022, Art. no. 2100891, doi: 10.1002/aelm.202100891.

[16] J. Y. Gerasimov et al., "An evolvable organic electrochemical transistor for neuromorphic applications," *Adv. Sci.*, vol. 6, no. 7, Apr. 2019, Art. no. 1801339, doi: 10.1002/advs.201801339.

[17] P. C. Harikesh et al., "Organic electrochemical neurons and synapses with ion mediated spiking," *Nature Commun.*, vol. 13, no. 1, p. 901, Feb. 2022, doi: 10.1038/s41467-022-28483-6.

[18] S. Pecqueur et al., "Neuromorphic time-dependent pattern classification with organic electrochemical transistor arrays," *Adv. Electron. Mater.*, vol. 4, no. 9, Sep. 2018, Art. no. 1800166, doi: 10.1002/aelm.201800166.

[19] M. Lukoševič ius and H. Jaeger, "Reservoir computing approaches to recurrent neural network training," *Comput. Sci. Rev.*, vol. 3, no. 3, pp. 127–149, Aug. 2009, doi: 10.1016/j.cosrev.2009.03.005.

[20] E. Donati, May 23, 2019, "EMG from forearm datasets for hand gestures recognition," *Zenodo*, doi: 10.5281/ZENODO.3194792.

[21] P. Gkoupidenis, D. A. Koutsouras, and G. G. Malliaras, "Neuromorphic device architectures with global connectivity through electrolyte gating," *Nature Commun.*, vol. 8, no. 1, p. 15448, May 2017, doi: 10.1038/ncomms15448.

[22] N. Garg, I. Balafrej, Y. Beilliard, D. Drouin, F. Alibart, and J. Rouat, "Signals to spikes for neuromorphic regulated reservoir computing and EMG hand gesture recognition," in *Proc. Int. Conf. Neuromorphic Syst.*, Knoxville, TN, USA, Jul. 2021, pp. 1–8, doi: 10.1145/3477145.3477267.

[23] S. Narayanan, M. Cartiglia, A. Rubino, C. Lego, C. Frenkel, and G. Indiveri, "SPAIC: A sub-μW/channel, 16-channel general-purpose event-based analog front-end with dual-mode encoders," 2023, *arXiv:2309.03221*.

[24] P. R. Paudel, V. Kaphle, D. Dahal, R. K. R. Krishnan, and B. Lüssem, "Tuning the transconductance of organic electrochemical transistors," *Adv. Funct. Mater.*, vol. 31, no. 3, Jan. 2021, Art. no. 2004939, doi: 10.1002/adfm.202004939.

[25] S. Pecqueur, D. Guérin, D. Vuillaume, and F. Alibart, "Cation discrimination in organic electrochemical transistors by dual frequency sensing," *Organic Electron.*, vol. 57, pp. 232–238, Jun. 2018, doi: 10.1016/j.orgel.2018.03.020.

[26] C. M. Proctor, J. Rivnay, and G. G. Malliaras, "Understanding volumetric capacitance in conducting polymers," *J. Polym. Sci. B, Polym. Phys.*, vol. 54, no. 15, pp. 1433–1436, Aug. 2016, doi: 10.1002/polb.24038.

[27] P. Leleux et al., "Organic electrochemical transistors for clinical applications," *Adv. Healthcare Mater.*, vol. 4, no. 1, pp. 142–147, Jan. 2015, doi: 10.1002/adhm.201400356.

[28] K. Janzakova et al., "Structural plasticity for neuromorphic networks with electropolymerized dendritic PEDOT connections," *Nature Commun.*, vol. 14, no. 1, p. 8143, Dec. 2023.

[29] R. L. Stoop, K. Thodkar, M. Sessolo, H. J. Bolink, C. Schönenberger, and M. Calame, "Charge noise in organic electrochemical transistors," *Phys. Rev. Appl.*, vol. 7, no. 1, Jan. 2017, Art. no. 014009.

[30] A. G. Polyravas et al., "Effect of channel thickness on noise in organic electrochemical transistors," *Appl. Phys. Lett.*, vol. 117, no. 7, Aug. 2020, Art. no. 073302, doi: 10.1063/5.0019693.

[31] C. Nathe, C. Pappu, N. A. Mecholsky, J. Hart, T. Carroll, and F. Sorrentino, "Resevoir computing with noise," *Chaos, Interdiscipl. J. Nonlinear Sci.*, vol. 33, no. 4, 2023, Art. no. 041101.

[32] M. Ghazal et al., "Electropolymerization processing of side-chain engineered EDOT for high performance microelectrode arrays," *Biosensors Bioelectron.*, vol. 237, Oct. 2023, Art. no. 115538, doi: 10.1016/j.bios.2023.115538.

Mahdi Ghazal received the M.Eng. degree in micro and nanotechnology engineering from the School of Engineering ESIEE PARIS, Paris, France, in 2019, and the Ph.D. degree in micro and nanoelectronics from the Institute of Electronics, Microelectronics and Nanotechnology (IEMN), Lille, France, in 2022.

Since 2023, he has been a Postdoctoral Researcher with IEMN. His research and technological interests during the Ph.D. and a Postdoctoral period include the study and development of organic nanoelectronics devices, such as microelectrode arrays and organic electrochemical transistors for interfacing and recording biological neurons. Part of his research has been carried out to develop organic polymer devices for neuromorphic engineering applications.

Ankush Kumar received the integrated Ph.D. (M.S.-Ph.D.) degree in materials science from the Jawaharlal Nehru Centre for Advanced Scientific Research, Bengaluru, India, in 2018. Further he did his first postdoctoral research from the Department of Mathematics, University of Pittsburgh, PA, USA, with a focus on synaptic plasticity in balanced cortical networks.

Since 2019, he has been a Postdoctoral Researcher with the Institute of Electronics, Microelectronics and Nanotechnology, CNRS, Lille, France, working on organic neuromorphic devices. He was also a Research Scholar at the Birck Nanotechnology Center, Purdue University, West Lafayette, IN, USA, and had research experience at the Center for Nano and Soft Matter Sciences, Bengaluru. Currently, he is a Postdoctoral Researcher with the Singapore University of Technology and Design (SUTD), Singapore, working on memristive networks. His research interests include neuromorphic systems, statistical modeling, materials and device designs, and networks and sensing.

Nikhil Garg received the B.Eng. degree in electrical and electronics engineering and the M.Sc. degree in biological sciences from the Birla Institute of Technology and Science Pilani, Pilani, India, in 2021.

From 2020 to 2021, he was a Research Assistant at the Interdisciplinary Institute for Technological Innovation (3IT), Sherbrooke, QC, Canada.

Since 2021, he has been a Doctorate with 3IT and IEMN, Lille, France. He works on engineering memristor-based neuromorphic hardware for edge AI applications in collaboration with Aix-Marseille University, Marseille, France, Paris-Saclay University, Gif-sur-Yvette, France, and IBM Research Zurich, Rüschlikon, Switzerland. His current research interests include neuromorphic computing, in-memory computing with emerging memory devices, and brain–computer interfaces.

Sébastien Pecqueur received the double M.Sc. degree in chemical engineering and inorganic chemistry from the National Graduate School of Physical Chemistry (ENSCPB), Bordeaux, France, and the University of Bordeaux, Bordeaux, in 2010, and the Ph.D. (Dr.-Ing.) degree in material sciences from Friedrich Alexander Erlangen-Nuremberg University, Erlangen, Germany, in 2014.

He is currently a Tenured Researcher with CNRS and the Institute for Electronics, Microelectronics and Nanotechnologies (IEMN), Villeneuve-d'Ascq, France. His main research interests include organic electronic materials and devices, and particularly their potential for future-emerging sensing technologies exploiting in materio information classification with organic electronic materials.

Fabien Alibart received the Ph.D. degree in material science from the University of Picardie Jules Verne, Amiens, France, in 2008.

In 2012, he joined IEMN-CNRS as a Permanent Researcher, where he worked on the concepts of neuromorphic/bio-inspired computing with emerging memory technologies. From 2017 to 2020, he was at LN2-3IT CNRS, Sherbrooke, QC, Canada, as a Researcher participating in the join laboratory program between France and Quebec (UMI-CNRS), where he was developing neuromorphic hardware for a variety of applications, from edge computing to brain–machine interfaces.

Dr. Alibart was a recipient of several projects, such as ERC-CoG IONOS. He was the Research Chair on neuromorphic engineering and computing from the Ministry of Economy and Innovation, QC, Canada. He is now pursuing research bridging neuromorphic computing concepts with neural cells interfaces.